Late Holocene seasonal and multicentennial hydroclimate variability in the Coorong Lagoon, South Australia: evidence from stable isotopes and trace element profiles of bivalve molluscs

Thesis submitted in accordance with the requirements of the University of Adelaide for an Honours Degree in Geology

Briony Kate Chamberlayne

November 2015

THE UNIVERSITY of ADELAIDE

LATE HOLOCENE SEASONAL AND MULTICENTENIAL HYDROCLIMATE VARIABILITY IN THE COORONG LAGOON, SOUTH AUSTRALIA: EVIDENCE FROM STABLE ISOTOPES AND TRACE ELEMENT PROFILES OF BIVALVE MOLLUSCS

RUNNING TITLE: PALAEOHYDROLOGY FROM MOLLUSC GEOCHEMISTRY

ABSTRACT

This study investigates the stable isotope and trace elemental geochemistry of the bivalve *Arthritica helmsi* with the aim to investigate its uses as a palaeoclimate archive. Firstly, stable isotopes and trace elements were measured on composite shell samples to create a long-term record of climate variability throughout the past 2500 years. Secondly, the seasonal variations within these multicentennial records was analysed through high-resolution trace elemental analyses on individual shells in addition to high replicate stable isotope analyses. These results show variation in the hydroclimate of the Southern Coorong Lagoon in response to freshwater flow and evaporation. A period of reduced moisture from 2200-1800 cal B.P and periods indicating more fresh conditions from 2500-2250 cal B.P and 1800-1300 cal B.P are in agreement with several other regional records suggesting a coherent regional climate signal. Increases in seasonality coincide with dry climates and indicate that summer climate variability is the main influence on Coorong palaeohydrology. *A helmsi* exhibits significant potential as a palaeoclimate tracer, subject to further research into it's contemporary biology and geochemistry.

KEYWORDS

Late Holocene

Coorong Lagoon

Arthritica helmsi

Climate Change

Oxygen isotopes

LA-ICP-MS

TABLE OF CONTENTS

LIST OF FIGURES AND TABLES

1. INTRODUCTION

Knowledge of past climate conditions is becoming increasingly important as we attempt to place recent change into perspective and create reliable models for the future (Snyder 2010). This is particularly important in Australia where the combination of a lack of regional palaeo-data (Neukom and Gergis 2011; Gergis *et al.* 2011) and short-lived climate records (Gergis *et al.* 2011) has resulted in a poor understanding of the long-term climate variability. Previous studies have had some success in reconstructing variability of rainfall (Saunders *et al.* 2012) and temperature (Fletcher and Thomas 2010; Saunders *et al.* 2013) of Australia in the Quaternary. However such studies are based on either remote proxies (Gergis *et al.* 2011) or proxies with a low temporal resolution, which may not adequately capture the dynamics of climate change at certain time frequencies. Moreover, studies investigating variability associated with the large scale climate phenomena – the El Niño-Southern Oscillation (ENSO) (Braganza *et al.* 2009; Gergis *et al.*), Indian Ocean Dipole (IOD) (Abram *et al.* 2007), Southern Annular Mode (SAM) (Hendon *et al.* 2007) and Interdecadal Pacific Oscillation (IPO) (McGregor *et al.* 2010; Gergis *et al.* 2011) - mostly rely on proxies from the wider pacific region and therefore are not directly representative of Australia's past climate.

One potential solution to the paucity of highly resolved terrestrial climate records in Australia is the geochemistry of bivalve molluscs. Bivalves grow by periodic accretion of calcium carbonate (Thompson *et al.* 1980), the geochemistry of which is determined by the temperature and isotopic composition of their growth waters (Urey 1947; Epstein *et al.* 1961). These growth increments represent approximately equal durations of time (Jones 1980; Witbaard *et al.* 1997) which depending on the species can be annual to daily (Wurster and Patterson 2001). This allows a unique perspective

not only on long-term climate variability but also on how patterns of seasonal climate variability evolve alongside long-term climate on multicentennial scales (Schöne and Fiebig 2009). As molluscs are widely distributed outside of the tropics and within the Southern Hemisphere (Schöne *et al.* 2005), sedimentary sequences containing abundant bivalves could potentially provide long-lasting composite climate records with extremely high temporal resolution in a region severely lacking in these types of data.

To date, stable isotope ratios of bivalves (in addition to annually banded gastropods and univalves) have been applied as proxies for temperature (Dettman *et al.* 2004), rainfall (Prendergast *et al.* 2015), ENSO variability (Carré *et al.* 2014), productivity (Wanamaker *et al.* 2009), upwelling (Ferguson *et al.* 2013) and river discharge (Versteegh *et al.* 2009). Trace element ratios have most successfully been used to reconstruct palaeotemperatures (Mg/Ca and Sr/Ca) and as palaeoproductivity meters (Ba/Ca) (Yan *et al.* 2014; Elliot *et al.* 2009). Na and Pb concentrations have also proven useful proxies for salinity and pollution (Findlater *et al.* 2014; O'Neil and Gillikin 2014).

This paper presents a record of 2500 years of climate variability in the Coorong region of South Australia constructed from the stable isotope and trace element profiles of bivalve molluscs. The ability to compare seasonality within the long- term low frequency response to global climate models such as ENSO is an exciting addition to palaeoclimate studies in the Southern Hemisphere that will facilitate a greater understanding of the climate and hydrological dynamics of the region.

2. BACKGROUND

2.1 Study site

The Coorong is a back-barrier lagoon system that extends > 130km southeast of the mouth of the Murray River along the coast (Figure 1). A narrow channel connects the Northern and Southern Lagoons, which are separated from the Southern Ocean by the Younghusband Peninsula. The Coorong receives freshwater inflow from the River Murray and marine input from the Southern Ocean through the mouth of the Murray River in addition to rainfall and surface/groundwater (Fluin *et al.* 2009; Geddes and Hall 1990).

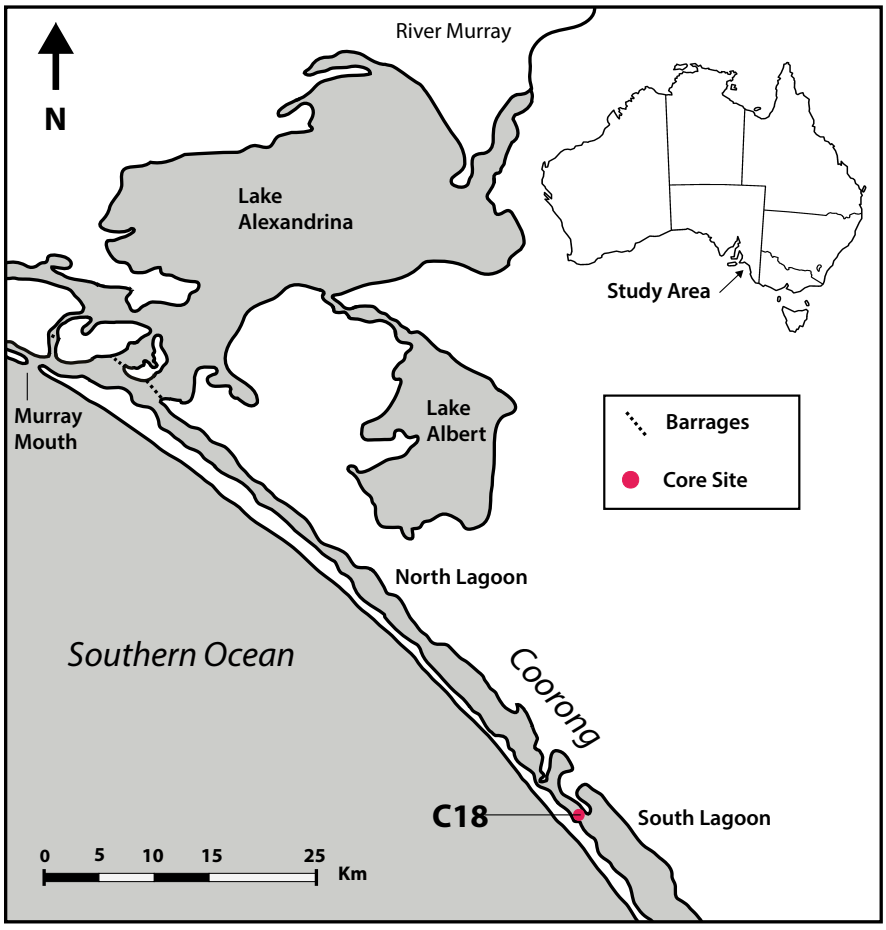

Figure 1. Map of the Coorong wetland in South Australia highlighting the location of core C18 in the Southern Lagoon.

The Coorong's estuarine lagoons are characterised by a significant salinity gradient, progressively becoming more saline as the distance from the Murray Mouth increases (Thomlinson 1996; Geddes and Hall 1990; Dittmann *et al.* 2013). In recent years the Northern Lagoon has been described as moderately hypermarine recording salinity values of 35-50‰ whereas in the Southern Lagoon values in the range of 80-110‰ indicate a strongly hypersaline environment (Geddes and Hall 1990; Dittmann *et al.* 2013). Studies show that these extreme modern salinities are a recent development (Thomlinson 1996; Tulipani *et al.* 2014) as before the introduction of barrages in 1940 salinities were unlikely to exceed seawater (36‰) in the northern lagoon and that the southern lagoon experienced fresher periods not observed today (Fluin *et al.* 2009).

Although the present geochemistry of the Lagoons is considered to be a result of interference with natural processes, there is evidence that the two Lagoons have been separate geochemical systems throughout the Late Quaternary (McKirdy *et al.* 2010). Fluin *et al.* (2009) in a diatom analysis of sediment cores from the Coorong found a lack of Murray River specific diatoms in the Southern Lagoon indicating that river flows did not penetrate into the Southern Lagoon during the Late Holocene. However, evidence for periods of freshening from cores further into the Southern Lagoon suggest that freshwater inputs from the south can be significant (Fluin *et al.* 2009).

2.2 Study species

The bivalve species used for all analyses in this study were identified as *Arthritica helmsi* (Hedley 1915) (Mollusca, Leptonidae) with the assistance of mollusc experts Winston Ponder (Australian Museum) and Thierry Laperousaz (South Australian Museum). Shells of *A. helmsi* can grow to approximately 3 mm from anterior

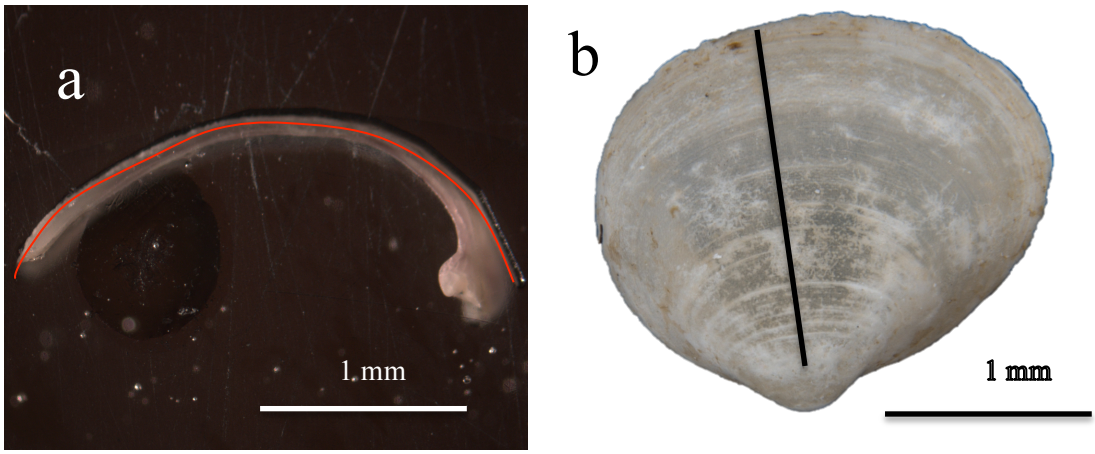

Figure 2. (a) *A. helmsi* shell sectioned through the maximum growth axis. The red line shows the location of a laser ablation transect parallel to the exterior growing surface. (b) *A. helmsi* shell highlighting the location of the maximum growth axis.

to posterior ends (Figure 2) and are generally found in the first 5 cm of sediments (Matthews and Constable 2004). *Arthritica* are filter feeders (Wells and Threlfall 1982) and breed their larvae before releasing crawling juveniles (Lautenschlager 2011). Little is known on the physiology of *A. helmsi*, including life span.

Common in estuarine systems of southeastern Australia (Lautenschlager 2011), *A. helmsi* can recruit steadily throughout the year (Wells and Threlfall 1982) as they are thought to have wide salinity and temperature tolerances (Lautenschlager 2011) although this range has not been quantified. Studies of this species in the Hopkins River estuary in Victoria, Australia, found no pronounced changes in their abundance during particular stages of the hydrological cycle, including increased freshwater input and the degree of openness of the estuary entrance (Lautenschlager 2011). Similarly, Matthews and Constable (2004) in a study of the same estuary found that *A. helmsi* experiences low mortality rates during increased freshwater discharge compared to other mollusc species.

Currently, populations of *A. helmsi* are re-establishing in the Murray Mouth and Coorong lagoons (Dittmann *et al.* 2013) after a recent absence presumably caused by

heightened salinity deemed unnatural in the scheme of the past 5000 years (Tulipani *et al.* 2014). Despite this recent absence, the marked abundance of shells in the sediments of the Coorong and their tolerance and growth ability through changing hydrological conditions suggests shells of *A. helmsi* could be useful as recorders of past hydrologic variability.

3. METHODS

3.1 Sample collection and preparation

A sediment core (core C18) was retrieved from the Southern Lagoon of the Coorong wetland in 2005 (Figure 1) by Deborah Haynes and colleagues. The coring site is proximal to the narrow channel connecting the Northern and Southern Lagoons (Figure 1). Shortly after collection, the core was sampled for preliminary diatom and radiocarbon analyses, but was otherwise stored intact, in the dark at 4°C until the commencement of this project. In April 2015 two attempts to sample the Southern Lagoon for living specimens to allow a modern calibration for this species were unsuccessful. However, modern samples collected from the Northern Lagoon and Murray mouth in February 2015 have since been obtained via Sabine Dittmann and colleagues at Flinders University, although not within the timeframe to allow their analyses to be included in this paper.

This core was selected both due to its geographical position at the confluence of the Northern and Southern Lagoons, but primarily due to the abundance of *Arthritica helmsi* shells throughout the core except for the uppermost 4 cm. The core was divided into 1 cm intervals which were freeze dried at -55°C for 24 hours. Shells for analysis were picked from the dried sediment and particulate matter was removed using a soft

brush and distilled water. To determine the mineralogy of this species, 1g of shells were collected and crushed into a fine powder using an agate mortar and pestle before being subjected to X-Ray Diffraction (XRD) analysis conducted qualitatively using a BrukeD8 ADVANCE Powder X-ray Diffractometer with a Cu-radiation source. Data was processed using Bruker DIFFRAC.EVA software and Crystallography Open Database reference patterns for identifying mineral phases.

3.2 Geochronology

Three preliminary radiocarbon dates for this core were available from the onset of this project. In addition to these, a further six dates were collected from samples consisting of five shells from samples spaced approximately 15 cm apart throughout the core. Radiocarbon analyses were conducted at the Australian Nuclear Science and Technology Organisation (ANSTO) using the STAR accelerator, funded via the Australian Institute of Nuclear Science and Technology (AINSE) Honours Scholarship Program. An age-depth model was developed in the CLAM program (version 2.2) in R (Blaauw 2010) for this core using a combination of new and previously obtained accelerator mass spectrometry (AMS) ^{14}C dates. The ^{14}C ages were calibrated against a mixed calibration curve consisting of the Marine (Reimer *et al.* 2013) and Southern Hemisphere (Hogg *et al.* 2013) ^{14}C master chronologies. The regional reservoir effect was defined as 62 ± 61 ^{14}C years as calculated from the weighted mean of the seven locations available for the region from the Marine Reservoir Correction Database (http://www.calib.qub.ac.uk/marine/). A smooth spline interpolation was selected for the construction of the age model and a smoothing factor of 0.3 chosen as the best fit for the calculated age constraints.

Table 1. Results from the AMS ^{14}C analyses used to construct the age model in CLAM (Blaauw 2010). Italicised samples were identified as outliers and excluded from the age model. Calibrated years BP (Cal yr BP) represents the 'best' estimation of calibrated age calculated in the age model where P=1950. Samples with prefix '-Wk' were dated at Waikato University, those with the prefix 'OZ' were dated at the Australian Nuclear Science and Technology Organisation (ANSTO) AMS facility (Fink *et al.* 2004).

Laboratory code	Sample type	Depth	$\delta^{13}C$ (‰)	pMC ± 1σ	^{14}C ± 1σ yr BP	Cal yr BP
OZS803	*Bivalve Carbonate*	*9-10*	*0.0**	*80.70 ± 0.22*	*1720 ± 25*	
OZS804	Bivalve Carbonate	20-21	0.0*	88.46 ± 0.24	985 ± 25	630
Wk-24750	*Bivalve Carbonate*	*30*	*0.4 ± 0.2*	*82.1 ± 0.2*	*1584 ± 30*	
OZS805	Bivalve Carbonate	45-46	0.3 ± 0.4	84.87 ± 0.25	1320± 25	1039
OZS806	Bivalve Carbonate	65-66	0.0 ± 0.1	81.26 ± 0.20	1665 ± 20	1359
Wk-24751	Bivalve Carbonate	82	0.4 ± 0.2	78.1 ± 0.1	1987 ± 30	1780
OZS807	Bivalve Carbonate	95-96	0.0*	73.97 ± 0.20	2420 ± 25	2135
OZS808	Bivalve Carbonate	115-116	1.2	72.10 ± 0.21	2630 ± 25	2466
Wk-24752	Bivalve Carbonate	129	0.7 ± 0.2	72.0 ± 0.2	2638 ± 30	2577

*** value is an estimated value**

3.3 Stable isotope analyses

Five pre-cleaned shells, collected at 1 cm intervals throughout core C18 were crushed to a fine powder using a mortar and pestle. A sub-sample of approximately 100 µg from this carbonate powder was used for stable isotope analysis. Samples were flushed with helium and then acidified with 100% phosphoric acid at 70°C before analysis on a Nu Instruments GasPrep in-line with a Nu Instruments Nu Horizon CF-Isotope Ratio Mass Spectrometer in continuous flow mode. Laboratory standards ANU-P3 ($\delta^{13}C$ = 2.2 ‰, $\delta^{18}O$ = -0.3‰) and UAC-1 ($\delta^{13}C$ = -15.0 ‰, $\delta^{18}O$ = -18.4‰) accounted for 27 each 100 analyses, the precision is better than 0.21‰ for $\delta^{18}O$ and 0.7‰ for $\delta^{13}C$ based on replicate analyses of these standards. To assess the degree of

intra-sample geochemical variability, multiple individual shells of *A. helmsi* were also analysed from depths of 11cm (n=30), 26 cm (n=29), 57cm (n=27), 92cm (n=30) and 119cm (n=27). Oxygen and carbon isotope data are reported as $\delta^{18}O$ and $\delta^{13}C$ respectively, relative to Vienna Pee Dee Belemnite (VPDB), as calculated in Equation 1.

$$\delta_x = \left(\frac{R_x}{R_s} - 1\right) * 1000 \qquad (1)$$

Where δ_x is the ratio of heavy to light isotope (e.g. $^{18}O/^{16}O$) and R_x and R_s are the ratios in the sample and standards respectively. δ_x values are reported in parts per thousand (permil) denoted as ‰.

3.4 Trace element analyses

3.4.1 SOLUTION ICP-MS

The elemental composition of multiple shell composites analysed for stable isotopes was determined using Solution Inductively Couples Plasma Mass Spectrometry (Solution ICP-MS). To do so, the phosphoric acid solution analysed for stable isotopes was diluted into 5mm of 70% nitric acid and analysed for trace elements using an Aligent 7500cs ICP-MS equipped with an Octopole Reaction System (ORS) at Adelaide Microscopy. Concentrations of ^{7}Li, ^{23}Na, ^{24}Mg, ^{27}Al, ^{39}K, ^{43}Ca, ^{55}Mn, ^{57}Fe, ^{59}Co, ^{63}Cu, ^{66}Zn, ^{85}Rb, ^{88}Sr, ^{95}Mo, ^{111}Cd, ^{118}Sn, ^{115}In, ^{138}Ba, ^{139}La, ^{140}Ce and ^{208}Pb were measured in addition to nitric acid standards to allow for correction of any drift. Average relative standard deviation (RSD, in %) considering all sequences (n=221) was 3.35% for Mg, 3.31% for Sr and 3.98% for Ba (for RSD of all elements measured see Appendix B).

3.4.2 LA-ICP-MS

In preparation for high-resolution trace elemental analysis, shells were embedded in indium spiked epoxy resin and cut along the maximum growth axis into ~500 μm sections using a low speed saw (Figure 2). These sections were polished in Millipore 18MΩ deionised water before being adhered to glass slides. Trace element ratios were measured on 4 shells from 12 cm depth, 8 shells from 30 cm, 50 cm, 70 cm, 89 cm and 110 cm depths and 21 shells from 21 cm depth using Laser Ablation Inductively Coupled Plasma Mass Spectrometry (LA-ICP-MS) at Adelaide Microscopy. Beam intensities of ^{7}Li, ^{23}Na, ^{24}Mg, ^{43}Ca, ^{44}Ca, ^{55}Mn, ^{57}Fe, ^{63}Cu, ^{88}Sr, ^{115}In, ^{138}Ba and ^{208}Pb were measured in a transect parallel to the exterior margin of the shell in the direction of growth (Figure 2). Ablation was achieved with a New Wave UP-213 laser ablation system using a pulse rate of 10 Hz, pulse energy of 50%, a spot size of 30 μm and plate movement of 10 μm/s with a He/Ar mixture as the ablation gas. Elemental analyses were performed on an Agilent 7500ce ICP-MS with a 10ms dwell time. ^{43}Ca was used as the internal standard and NIST 612 as an external standard (Pearce *et al.* 1997) in addition to a laboratory carbonate standard MACS. Average relative standard deviations were 2.54 % for Mg, 1.36 for Sr and 0.779 for Ba (for RSD of other elements see Appendix B).

LA-ICP-MS data was processed using the GLITTER© software (van Achterbergh *et al.* 2001). For signal integration, the background was identified and subtracted from the stable signal. Quantitative element concentrations were calculated from the external standard NIST 612.

4. RESULTS

4.1 Mineralogy

Figure 3 shows the XRD pattern obtained from the bulk sample of *A. helmsi* carbonate. The peaks correspond in intensity and spacing to the 2θ angles of XRD peaks of aragonite and showed no evidence for the presence of other carbonate phases.

4.2 Geochronology

The results of six newly obtained radiocarbon dates in addition to three previously obtained analyses are summarised in Table 1. An age-depth curve (Figure 4) was constructed using the 'best' estimation of calibrated ages following calibration of the measured ^{14}C dates in CLAM (Blaauw 2010). Of the nine radiocarbon samples measured

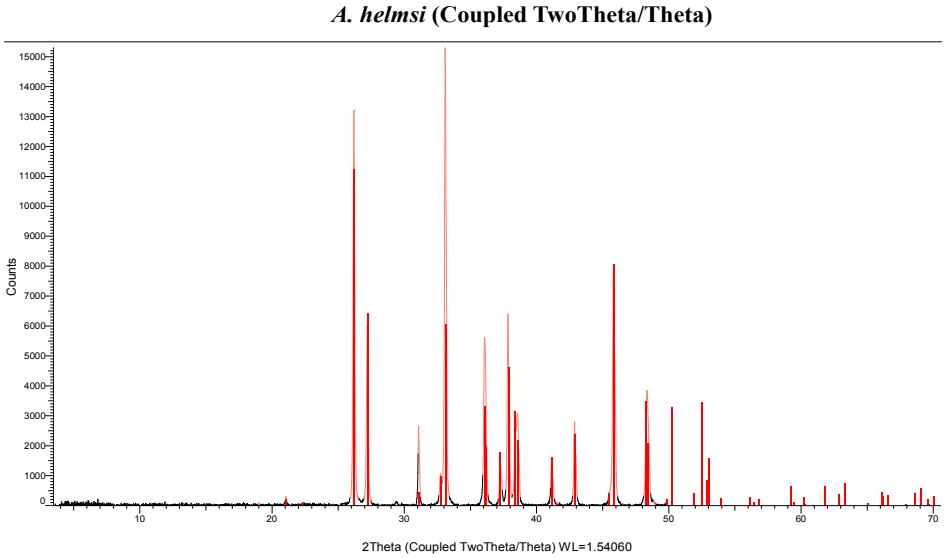

Figure 3. XRD results from a carbonate powder comprised of multiple *A. helmsi*. The black peaks are from the sample and the red show the signal for pure aragonite.

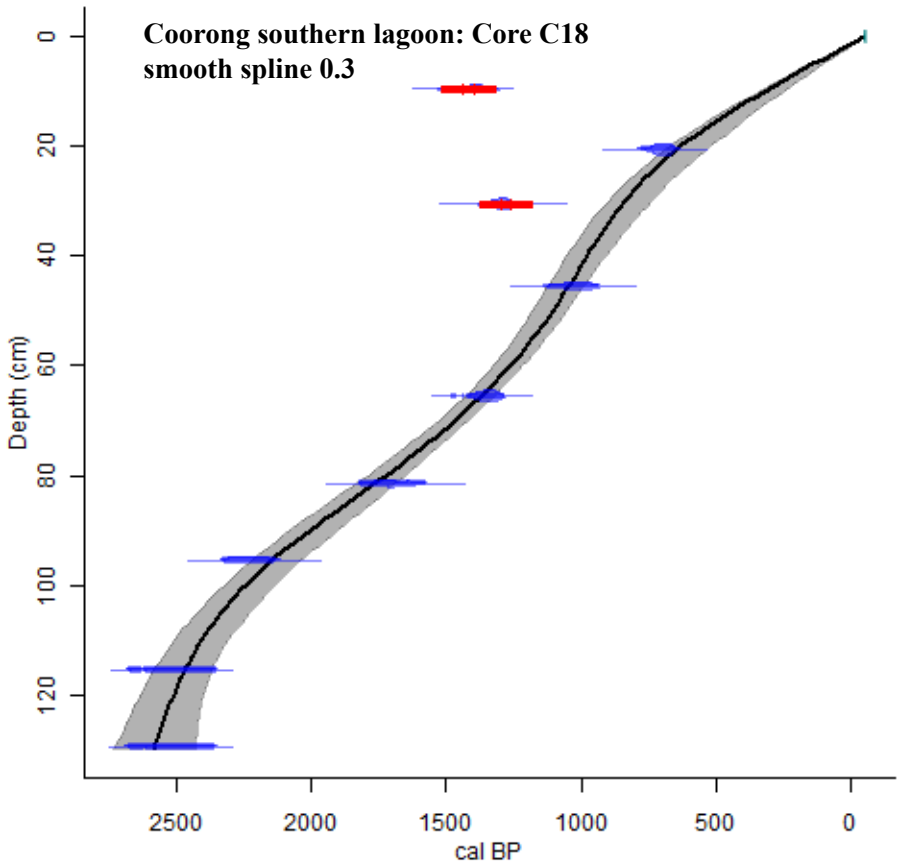

Figure 4. Age depth model the southern Coorong lagoon derived from radiocarbon ages of shells in core C18. The red points have been rejected as outliers and were not included in the calibration. Black line represents a 0.3 span spline fit and the grey shaded area represents a 95% confidence interval.

from core C18, two samples (9-10cm and 30cm) fall significantly outside the trend and were excluded as outliers from the age-depth model. The age model (Figure 4) indicates a reasonably linear sedimentation rate of approximately 20 cm/year and presents a mean basal age for core C18 of 2577 calibrated years before present, where present = CE 1950 (cal. B.P.). There were no obvious differences between the age-depth relationships of the three preliminary dates and those collected through this study.

4.3 Stable Isotopes

The results of stable oxygen and carbon isotope analyses of multiple shell composites and individual shells of *A. helmsi* from core C18 are shown in Figure 5 (details in appendix A). Following the results of the XRD analysis, all results are corrected to aragonite following the fractionation factors described by

Lécuyer *et al.* (2012). The values obtained from each centimetre of the core (n=124) represent on average an approximately 20-year window. The $\delta^{18}O$ of shell aragonite ($\delta^{18}O_{shell}$) throughout the core ranged from 3.7‰ to 5.67‰ with an average and standard deviation of -0.342‰ ± 0.428‰. The $\delta^{13}C$ of shell aragonite ($\delta^{13}C_{shell}$) ranged from -1.42‰ to 1.57‰ with an average and standard deviation of 0.607‰ ± 0.555‰. Figure 5 shows two periods of prolonged enrichment in $\delta^{18}O_{shell}$ from ~2200-1750cal. B.P. and from ~ 600-137 years cal. B.P. in addition to a peak ~1300 cal. B.P. Relative depletion is evident from ~1200-1100 cal. B.P. and 1700-1500 cal. B.P. $\delta^{13}C_{shell}$ is relatively enriched between 1250 and 700 years cal. B.P. before a period of depletion from 600-137 years cal. B.P. Correlation between $\delta^{18}O_{shell}$ and $\delta^{13}C_{shell}$ throughout the core is highly variable, both strong positive and negative correlations occur within the record (Figure 7).

Table 2. Mean standard deviations of stable oxygen and carbon isotopes measured on individual shells of *A. helmsi* ($\delta^{18}O_{(individuals)}$ and $\delta^{13}C_{(individuals)}$). For individual shell values data see appendix A. All isotope values are in ‰ relative to VPDB.

Depth	Number of samples	Mean $\delta^{18}O_{(individuals)}$	Standard deviation $\delta^{18}O_{(individuals)}$	Mean $\delta^{13}C_{(individuals)}$	Standard deviation $\delta^{13}C_{(individuals)}$
11	27	3.98	0.413	-0.543	0.696
26	26	3.88	0.486	-0.427	0.619
57	25	3.91	0.650	-0.331	1.06
92	26	4.38	0.391	-0.18	0.777
119	27	4.68	0.705	-0.484	0.730

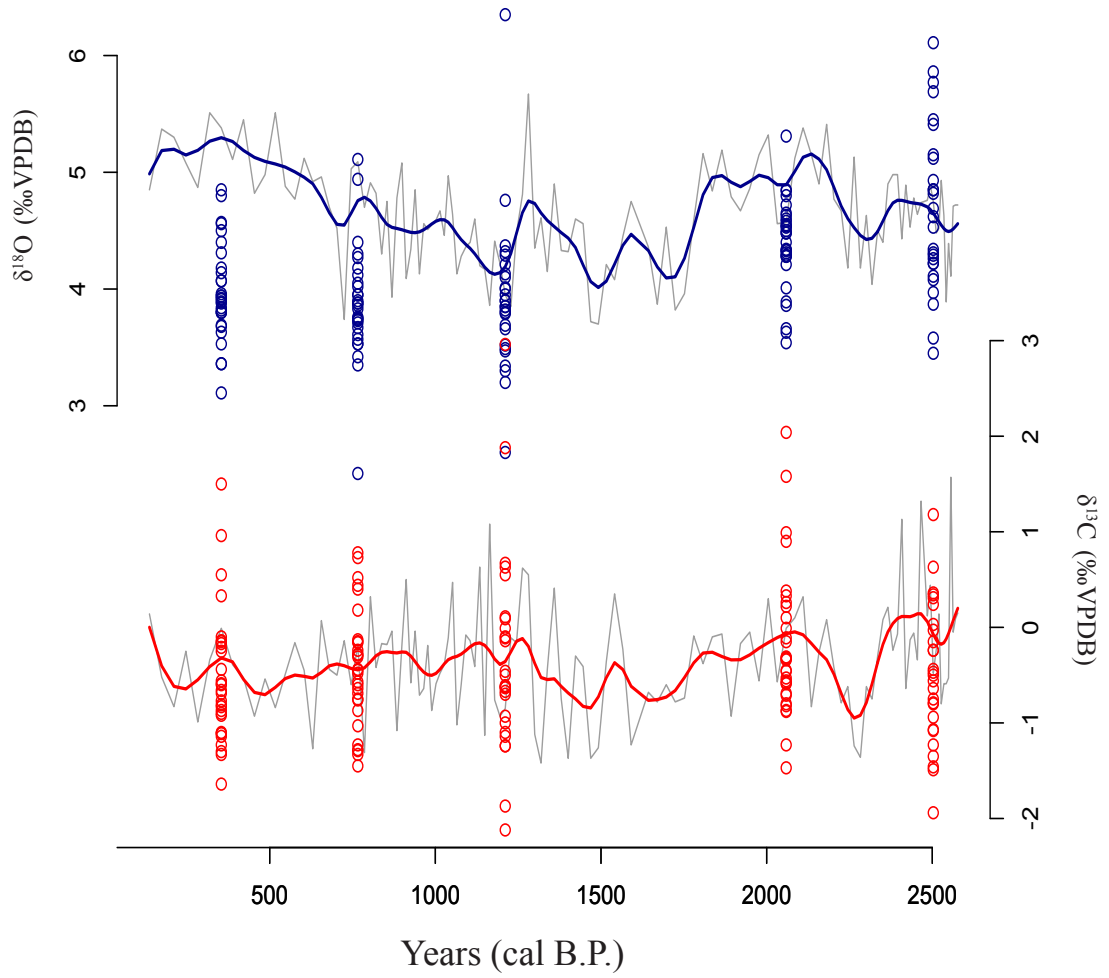

Figure 5. $\delta^{18}O$ and $\delta^{13}C$ through time as measured on bulk samples of *A. helmsi* from the Coorong's southern lagoon. $\delta^{18}O$ and $\delta^{13}C$ of individual *A. helmsi* (open circles) are measured from shells from 11cm (n=30), 26 cm (n=29), 57cm (n=27), 92cm (n=30) and 119cm (n=27). The grey line represents a measurement from each centimetre of core C18 and the blue and red lines represent a smooth spline (df=30) of this data for oxygen and carbon respectively.

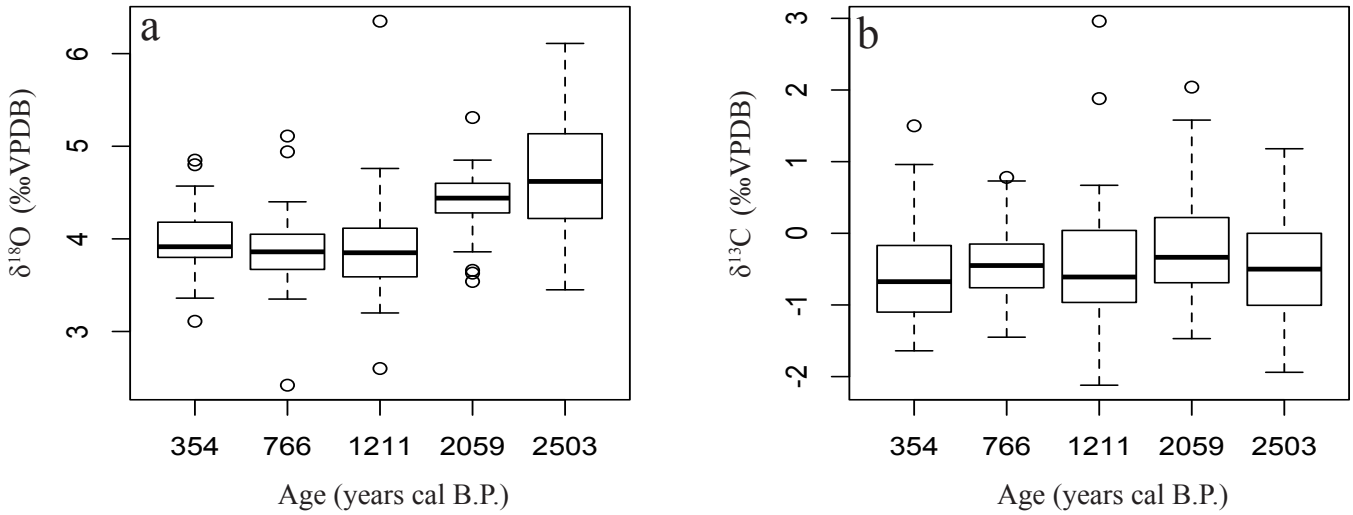

Figure 6. Box and whisker plots of $\delta^{18}O$ (a) and $\delta^{13}C$ (b). Values are obtained from multiple individual shell analyses of shells aged 354 years (n=30), 766 years (n-29), 1211 years (n=27), 2059 years (n=30) and 2503 years (n=27).

Individuals of *A. helmsi* were analysed from 5 depths within the core to investigate variance within each 1cm interval (Figure 5). $\delta^{18}O$ data from 57 cm, 92 cm and 119 cm bracket the composite shell data as expected while the $\delta^{18}O_{shell}$ data from 11 cm and 26 cm plot significantly below both the corresponding 5-shell composite measurement and the smoothed curve of the data (Figure 5). Individuals from 119 cm depth show the highest mean and standard deviation in $\delta^{18}O_{shell}$ (4.68‰ ± 0.705‰) while the smallest standard deviation (0.391‰) occurred in samples from 92 cm, which also had a comparatively high mean $\delta^{18}O_{shell}$ value (4.38‰). The variance within $\delta^{13}C_{shell}$ measurements is high for all depths with a minimum of 0.619‰ at 26 cm. The standard deviation of $\delta^{13}C_{shell}$ is highest in the 92 cm depth interval (0.777‰), while the $\delta^{18}O_{shell}$ measurements from this stratigraphic level record the lowest standard deviation (0.391‰) (Table 2; Figure 6).

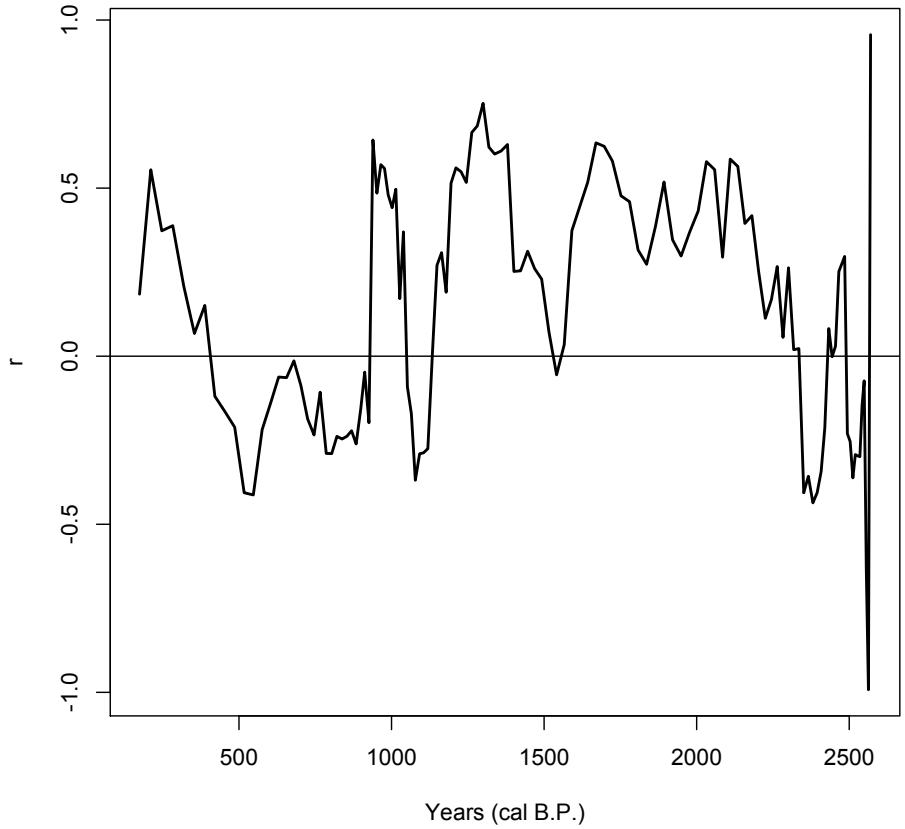

Figure 7. The Pearson product-correlation coefficient between $\delta^{18}O$ and $\delta^{13}C$ in composite samples of *A. helmsi* thought core C18. An r value 1 is a perfect positive correlation and an r value of -1 is a perfect negative correlation. Curve is a ~200 year running correlation.

4.4 Trace elements

4.4.1 SOLUTION ICP-MS

The concentrations of several trace elements were measured on the 5-shell composite carbonate powders that were also analysed for stable isotope ratios. The concentrations of Mg, Sr and Ba throughout core C18 are shown in Figure (7). Focus is placed on these elements as they show variable patterns and are commonly employed as environmental proxies in the literature (Elliot *et al.* 2009; Schöne *et al.* 2013; Lazareth *et al.* 2003). Mg/Ca has an average of 1.66 mmol/mol and a range of 0.84- 5.45 mmol/mol; Sr/Ca an average of 2.60 mmol/mol and range of 1.89 – 3.72 mmol/mol; and Ba/Ca an average of 0.0925 and a range of 0.0271 mmol/mol.

4.4.2 LA-ICP-MS

LA-ICP-MS profiles across the growth direction along the outer edge of *A. helmsi* were completed on 65 shells from 7 depths within the core. Any shells for which the In values were consistently elevated or the ablation line was visually determined to have missed the shell were excluded resulting in 36 shells for discussion (see appendix B for details). Majority of scans showed one or two distinct peaks in Mg/Ca, Sr/Ca and Ba/Ca as per the profile shown in Figure 10. These three trace element ratios show similar patterns along the length of the shell, particularly between Sr/Ca and Ba/Ca (R^2= 0.72). Mg/Ca shows a significant but less powerful correlation with Sr/Ca and Ba/Ca (R^2= 0.32 and R^2= 0.27 respectively). Any peaks that corresponded with high indium levels were removed from the analysis, as they are not representative of the shell carbonate.

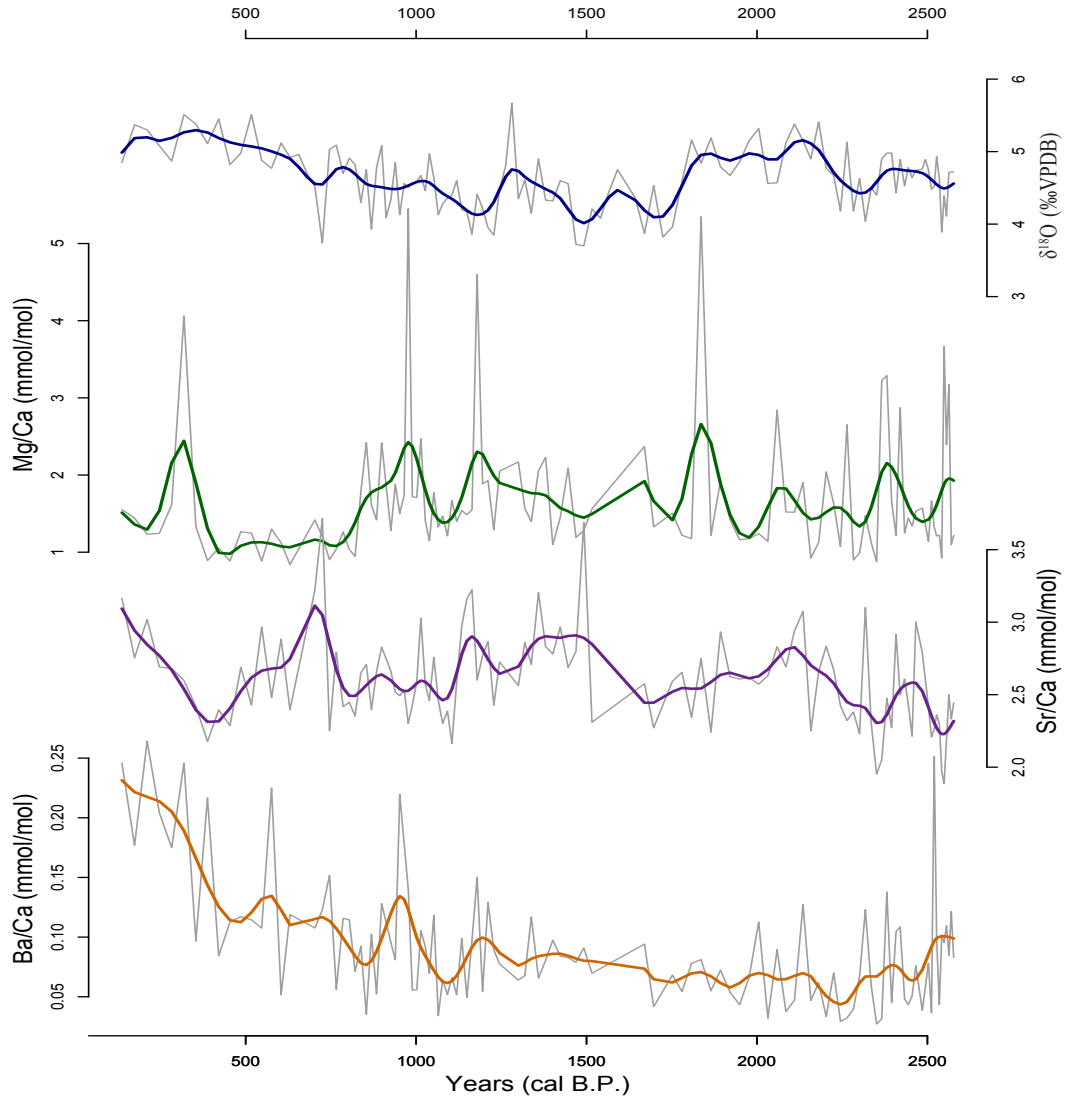

Figure 8. $\delta^{18}O$, Mg/Ca, Sr/Ca and Ba/Ca measured from composite samples of *A. helmsi* from each cm (~20 years cal B.P.). Grey lines represent raw data and the coloured lines represent a smooth spline (df=30).

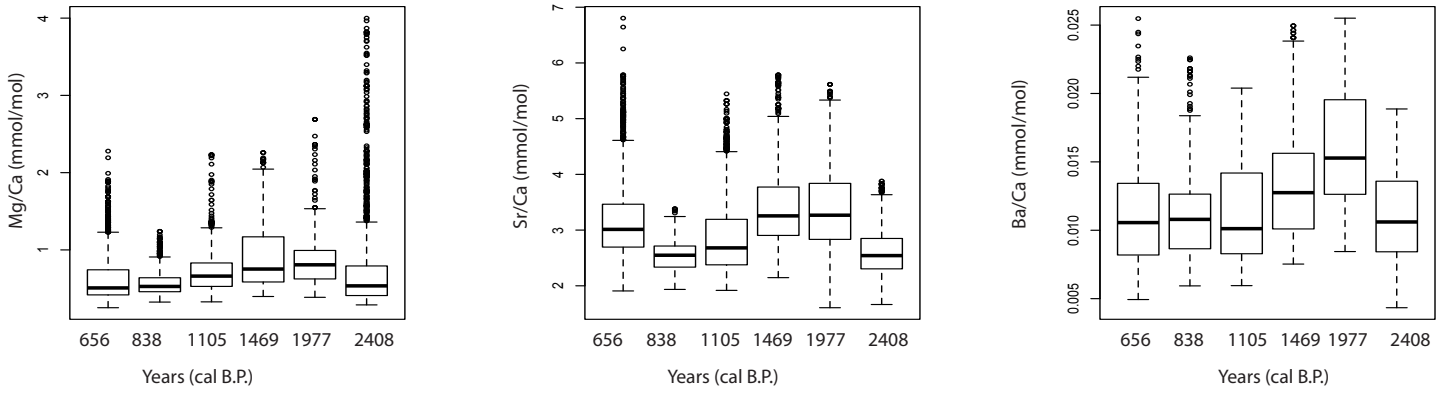

Figure 9. Box and whisker plots of trace element values of individual shells of *A. helmsi* from six depths within core C18.

The range of Mg, Sr and Ba values determined by LA-ICP-MS are highly variable both within and between depth intervals (Figure 9). The maximum values within depth intervals are particularly varied for all element ratios while the minimum and median values are less so – particularly in the Mg/Ca ratios. Mg/Ca shows an extremely varied range of values from 2408 years cal. B.P. (mean= 0.742 ± 0.587 mmol/mol) while this is less pronounced in Sr/Ca and Ba/Ca (mean = 2.6 ± 0.427 and mean = 0.0109 ± 0.00313 respectively). The range is high for all element ratios for 656 years cal. B.P. and reduced at 838 years cal. B.P. (Figure 9).

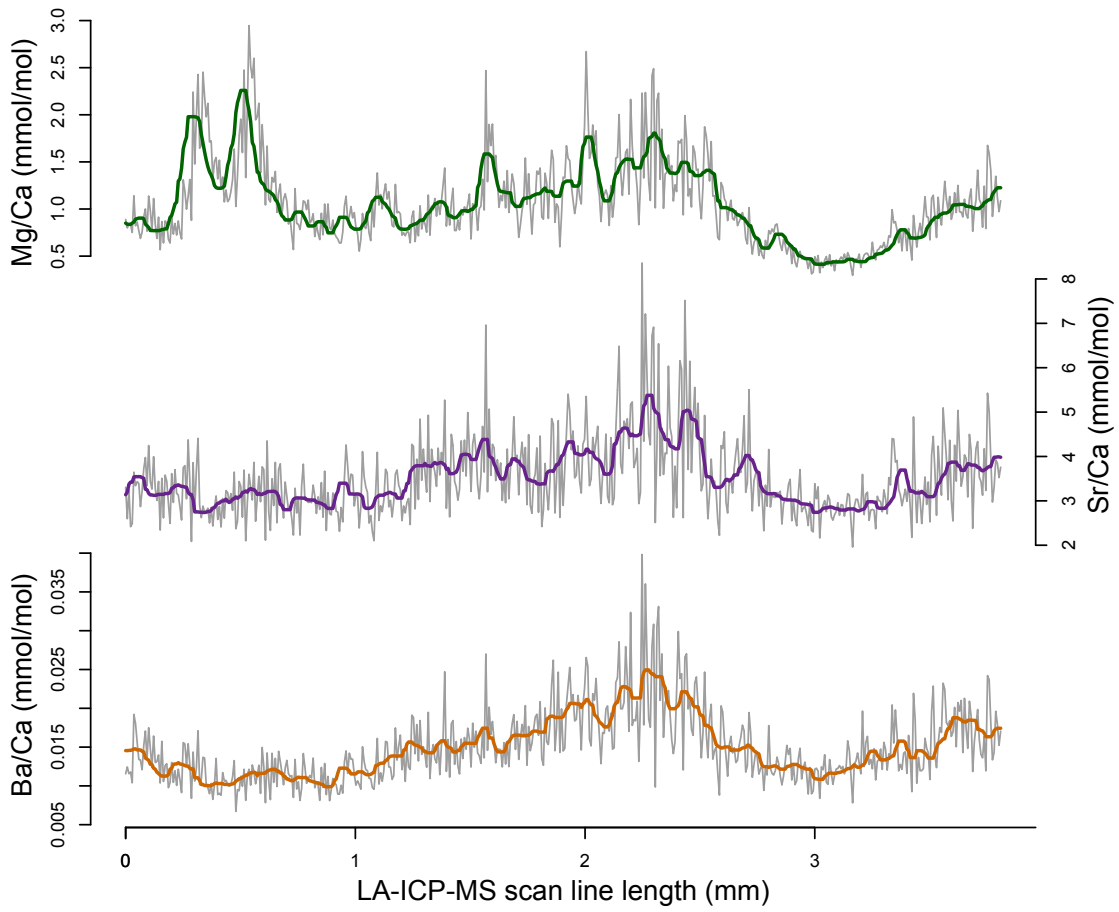

Figure 10. Trace element profiles from a single LA-ICP-MS of an individual *A. helmsi*. Coloured lines are a 7-point running median of the raw element ratios depicted by the grey lines.

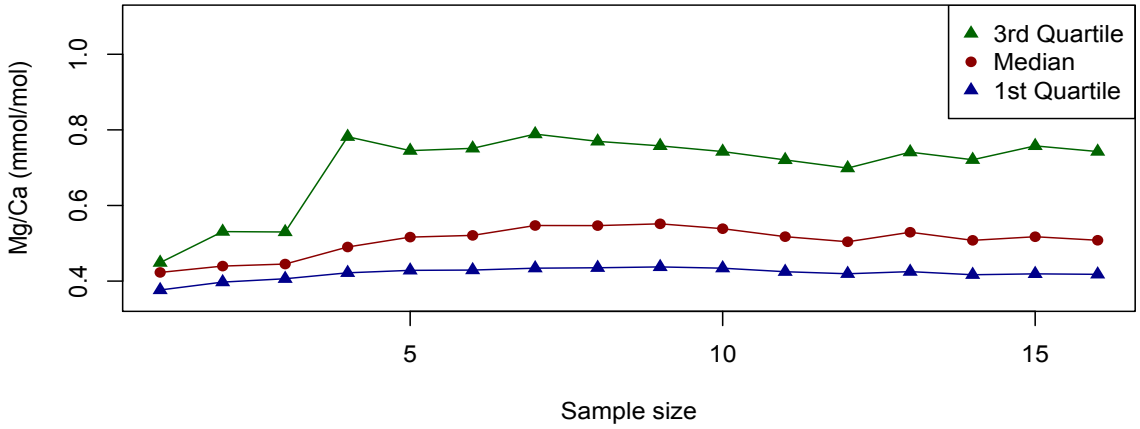

Figure 11. Mg/Ca ratio median and quartile ranges for shells from 21 cm depth (656 years cal B.P.).

To assess the number of individual shells needed to produce a reliable average in each age increment a high replicate LA-ICP-MS analysis was undertaken for the 21-22 cm interval (n=16; age= 656 years cal. B.P.). The median and 1st and 3rd quartiles from aggregated data increasing in sample size shown in Figure 11. All three statistics increase in value from 1-5 analyses and plateau from 5-16 analyses, although some small variation still occurs in this range.

5. DISCUSSION

5.1 Palaeohydrology of the Southern Coorong Lagoon

5.1.1 EVIDENCE FROM STABLE ISOTOPES

A stable isotope record based on multiple shell composites from approximately each 20 years of sediment from core C18 reveals long periods of enrichment and depletion in both $\delta^{18}O$ and $\delta^{13}C$, although these periods are not always correlated in time. While some studies show good correlation between these two tracers (Koutavas *et*

al. 2006) the relationship in this study is not clear (Figure 7), possibly due to differing controls on their integration in shell carbonate. The $\delta^{18}O$ of calcium carbonate is controlled by the temperature and oxygen isotopic concentration of the water from which it is precipitated (Urey 1947; Epstein *et al.* 1961) in addition to the vital effects related to the physiology of the carbonate biosynthesiser concerned (Schöne *et al.* 2013). While a number of studies have successfully applied this relationship to create long lived temperature reconstructions (Butler *et al.* 2013) these studies are based on well-studied marine bivalves and so the relationship between biological effects, temperature and $\delta^{18}O_{shell}$ is simplified by the ability to calculate water $\delta^{18}O$ and the knowledge of the shells physiology (Schöne and Surge 2014). In an estuarine system such as the Coorong, this relationship is complicated as the primary control on the $\delta^{18}O$ of the water is the mixing of marine and freshwater inputs in addition to evaporation. In addition, this study represents the first measurements of the isotopic composition of *A. helmsi*, and that to date, living specimens of this species have not been studied severely limiting our knowledge on the species-specific fractionation factors. Nevertheless, semi-qualitative hydrological reconstructions are viable and applied here through the analysis of isotope data for *A. helmsi.*

As salinity shows linear correlations with both the $\delta^{18}O$ of shells and water in lagoonal environments (Sampei *et al.* 2005) it is proposed that variation in the oxygen isotopic values in shells are indicative of changes in evaporation and freshwater flows in the Coorong Lagoons. The $\delta^{18}O$ analyses from composite shell samples therefore provide a time series of hydrological change at ~20 year intervals. These data suggest that a sustained period of increased evaporation and dryness was experienced from ~ 2200-1800 years cal. B.P in addition to a brief dry event at ~ 1250 years cal. B.P.

Periods of relative depletion in $\delta^{18}O$ from ~2500-2250 years cal. B.P, ~1800-1300 years cal B.P and ~1250-1000 years cal B.P suggest cooler less evaporative conditions during these times. The period from 1000-100 years cal. B.P shows significant disparity between the composite shell data and the single shell analyses which is possibly due to a technical problem related to calibration outside the range of available standards. Further research is needed to ascertain the origin of this disparity. For this study, this data will be excluded from the discussion; with the $\delta^{18}O$ record effectively ending at 1000 cal B.P. Interpretation of the $\delta^{13}C$ from this record is more challenging as the determinants of carbon stable isotope ratios in aragonitic shells are poorly understood (Butler *et al.* 2011). Gillikin *et al.* (2006) excluded the use of $\delta^{13}C$ as a robust proxy for salinity or the isotopic composition of dissolved inorganic carbon ($\delta^{13}C_{DIC}$) due to the unpredictable relationships between organic and inorganic pools of dissolved carbon. Furthermore the shells food source, biological controls and proportions of metabolic carbon can further complicate these interpretations (Elliot *et al.* 2009; Gillikin *et al.* 2006). The highly variable correlation between $\delta^{18}O$ and $\delta^{13}C$ from these analyses (Figure 7) support that $\delta^{13}C$ is enigmatic in bivalve shells. The species-specific determinants of shell $\delta^{13}C$ therefore require further detailed investigation prior to interpretation.

As an alternate approach to examining changes in seasonality through time, multiple replicate shells were analysed for their stable isotope compositions. Similar studies using short lived biogenic carbonates have been carried out by Koutavas *et al.* (2006), Carré *et al.* (2013) Dixit *et al.* (2015) to infer changes in ENSO, ocean temperature seasonality and the seasonal $\delta^{18}O$ and temperature of lakes. The range of $\delta^{18}O$ values obtained via the analysis of multiple individuals is widest at 1211 years cal.

B.P. and 2503 years cal B.P. when the $\delta^{18}O$ of the composite analysis indicates periods of cooler wetter conditions (Figure 6). The range of values from 2059 years cal B.P. show considerably less variation despite corresponding with a dry evaporative period according to the composite curve (Figure 6). This is in disagreement with previous studies that indicate that variability is increased when dry climates (Koutavas *et al.* 2006). However Dixit *et al.* (2015) suggested from their study that high intra-sample $\delta^{18}O$ variability could be caused by large seasonal changes in evaporation/precipitation for which signal could be obscured by a moderate average value. This could be the case for this study where moderate $\delta^{18}O$ values in the composite samples is a result of averaging amplified minimum and maximum values in individuals.

Although the ability to capture the seasonal range of $\delta^{18}O$ in the Coorong Lagoon relies on *A. helmsi* being able to tolerate and record seasonal extremes, the wide range of values measured for this species (particularly $\delta^{18}O$ at almost $4^{0}/_{00}$) support this assumption. Because the duration and influences on growth in *A. helmsi* are unknown, it is possible that there are growth hiatus' or that growth rates are not continuous throughout the year, which could also result in a seasonal bias. However, visual examination of the shells under cross section, using both light and scanning electron microscopy, revealed no marked changes in the colour or crystal structure of the aragonite. It is therefore inferred that growth hiatuses did not occur during the life cycles of the bivalves studied, however future research should look to examine the seasonal growth patterns of *A. helmsi* and their seasonal geochemical properties in shells to verify the conclusions made in this study.

5.1.2 EVIDENCE FROM TRACE ELEMENTS

A variety of studies have examined the trace elements of coastal molluscs (Lazareth *et al.* 2003; Carré *et al.* 2006), the majority of which to investigate whether Mg/Ca, Sr/Ca and Ba/Ca are reliable palaeothermometers. Despite the growing body of literature in this field, no consensus has been reached on the utility of these elemental ratios as proxies for environmental change. For example, (Lazareth *et al.* 2013) found that while Mg/Ca incorporation was controlled by the age of the shell, Sr/Ca and Ba/Ca could be used as reliable environmental proxies. In contrast, (Elliot *et al.* 2009) found that Mg/Ca had a temperature control in aragonitic shells and that Sr/Ca and Ba/Ca were not controlled by temperature. Studies have reported various vital effects as controls of both Mg/Ca uptake (Surge and Lohmann 2008) and Sr/Ca uptake (Gillikin *et al.* 2006) highlighting the need for species-specific determination of the controls of trace element incorporation in bivalve shells. For the following discussion, increases in trace element ratios will be interpreted as indicators of increased estuarine salinity (Paoulain *et al.* 2015) as caused by increased evaporation and reduced freshwater inputs.

Trace element concentrations were measured on 5-shell composite samples of *A. helmsi* from throughout core C18 to create a time-series of geochemical variation. Mg/Ca, Sr/Ca and Ba/Ca show little similarity throughout the 2500-year record. A sustained period of low Mg/Ca values from ~1000-500 years cal B.P. suggests stability in salinity and the lake level while Sr/Ca shows decreasing salinity and Ba/Ca shows a steep increase salinity during the same time period (Figure 8). This record shows little coherence and without disentangling the species specific factors influencing these values, this record is difficult to interpret in a palaeohydrological sense.

LA-ICP-MS trace element profiles of individual shells indicate *A. helmsi* have a potential to resolve seasonal climate. Element profiles of individual shells display peaks and troughs thought to be seasonal oscillations throughout the growth history of the shell (Figure 10). One to two peaks in this pattern can be observed in a single shell suggesting that one to two seasonal cycles may be captured in the shell geochemistry. The element profiles are continuous providing further support to the continuous growth of *A. helmsi.* Correlation between the Mg, Sr and Ba ratios in these shells suggests that a common driver influences these concentrations (Elliot *et al.* 2009). However, modern controls on trace element uptake into *A. helmsi* has not been undertaken, it is difficult to accurately interpret what this driver may be.

The trace element ratios of multiple shells from 6 depth intervals in the core were analysed providing a measure of the amplitude and variability of the seasonal cycle within the deposition window (~20 years). Both Mg/Ca and Ba/Ca individual measurements plot within the range observed from the same ratios in the composite curve. Sr/Ca however plots higher on average and many data points lie outside the range measured in Solution ICP-MS. A possible explanation for this is Sr/Ca heterogeneity in the aragonite; this is reported for several other bivalve species (Schöne *et al.* 2013).

The trend observed in trace element variability through time indicates heightened seasonal amplitude in the Southern Coorong Lagoon at 1977 years cal B.P., 1105 years cal B.P., and 656 cal B.P. and a reduction in seasonality at 2408 years cal B.P and 838 years cal B.P. Depth intervals with reduced range also show reduced median values. This in combination with the contrast in variation of maxima and minima between the different depth intervals suggests that changes in seasonality greater impact summer maximums than winter minimums in this environment.

To assess how many analyses from a 1cm interval would be sufficient to capture an accurate picture of the variation within that time slice, a high replicate analysis of shells from 21cm (656 years cal B.P.) was performed. Figure 11 indicates that at least more than 5 shells from each depth would be required to make robust conclusions regarding the median and range of values for a certain interval of time. Less than 5 shells were included in the analysis of trace element variance in shells from 30 cm, 70 cm and 89 cm and so further analyses should be conducted to improve the reliability of this data.

5.2 Regional implications

The hydroclimate variability in the Southern Coorong Lagoon inferred from a $\delta^{18}O$ record of composite shell samples shows similarities with hydrologic reconstructions from Victoria and southeastern South Australia suggesting a regionally coherent pattern of climate change (Barr *et al.* 2014 Kemp, Moros; Kemp *et al.* 2012; Moros *et al.* 2009). However, one notably different record is the Blue Lake, Mt. Gambier (Gouramanis *et al.* 2010). Reasons for this disparity could be due to the significant differences in lake morphology (The Blue Lake is >60 m deep and is fed by groundwater) or due to the poor resolution of data and inaccuracies in dating.

Two methods were employed to infer seasonality within the long-term climate trends. The ability of *A. helmsi* to capture the seasonal range in trace element ratios was shown to be successful indicating that seasonality is increased at times of high evaporation (inferred from the composite $\delta^{18}O$ record). Contrastingly, variation in $\delta^{18}O$ of multiple individuals of *A. helmsi* indicate do not show increased seasonality in

relation to inferred periods of dry evaporative conditions. The disagreement in these records may be due to the controls on the uptake of stable isotopes and trace elements in shells, as unlike $\delta^{18}O_{shell}$ the trace element ratios of shells are not influenced by the stable isotopes of water (Schöne *et al.* 2010). Modern studies could aid in resolving this disagreement.

A. helmsi hold great potential as an archive of past climate variability as while they are short-lived they are abundant in sediments and record trace element and stable isotope geochemistry throughout their lifetime. However, to move forward in this research, modern studies must be carried out to determine the vital effects of *A. helmsi*. Aspects including the growth patterns, life span, incorporation of elements and correlation with climate/ water chemistry data must be resolved to begin to create quantitative climate records.

6. CONCLUSIONS

1. Studies of seasonal climate and environmental change over multidecadal time scales is crucial to understanding the dynamics of long term climate variability. This is particularly important in Australia and the southern hemisphere where a lack of long-lasting high-resolution climate records is impairing our understanding of natural climate systems.

2. Bivalve molluscs hold great potential to study such dynamics. The shells of *A. helmsi* are abundant within stratigraphically constrained sediments, and appear to hold promise for palaeoclimate research.

3. The geochemistry of A. helmsi revealed a record of salinity and evaporation in the Southern Coorong Lagoon. The ~2500 year $\delta^{18}O$ showed periods of increased evaporation and salinity from 2200 – 1800 cal B.P. and gave evidence for periods of greater freshwater input and reduced evaporation from 2500-2250 cal B.P. and 1800-1300 cal B.P.

4. Seasonality was demonstrated to be variable throughout the record. Seasonality inferred from trace element ratios of individual shells indicate that during periods of reduced freshwater input and increased evaporation (enriched $\delta^{18}O_{shell}$) seasonality was increased and particular variation occurred in the maximum values. This suggests that summer variation is most responsible for long-term climate and hydrological variability in the Coorong.

ACKNOWLEDGMENTS

I would like to thank supervisors Jonathan Tyler and Bronwyn Gillanders for their support, guidance and encouragement. Christopher Izzo for his assistance with data processing and his advice. Deborah Haynes supplying the sediment core and preliminary radiocarbon dates for this project along with her comments. John Tibby for discussions. Geraldine Jacobsen at ANSTO for performing the radiocarbon analysis and AINSE for providing the funding to do so through their Honours Scholarship Program. Mark Rollog for his assistance and expertise in IRMS analyses. Aoife McFadden and Ben Wade from Adelaide Microscopy for their guidance with Solution ICP-MS and LA-ICP-MS analyses. Thierry Laperousaz (South Australian Museum) and Winston Ponder (Australian Museum) for their assistance with species identification and Sabine Dittmann and Ryan Barring at Flinders University for supplying modern shell samples.

This research is supported by the AINSE honours scholarship program.

REFERENCES

ABRAM N. J., GAGAN M. K., LIU Z., HANTORO W. S., MCCULLOCH M. & SUWARGADI B. W. 2007 Seasonal characteristics of the Indian Ocean Dipole during the Holocene epoch, *Nature,* vol. 445, pp. 229-302.

BARR C., TIBBY J., GELL P., TYLER J., ZAWADZKI A. & JACOBSEN G. E. 2014 Climate variability in south-eastern Australia over the last 1500 years inferred from the high-resolution diatom records of two crater lakes, *Quaternary Science Reviews,* vol. 95, pp. 115-131.

BLAAUW M. 2010 Methods and code for 'classical' age-modelling of radiocarbon sequences, *Quarternary Geochronology,* vol. 5, pp. 512-518.

BRAGANZA K., GERGIS J., POWER S., RISBEY J. & FOWLER A. 2009 A multiproxy index of the El Nino-Southern Oscillation, A.D. 1525-1982, *Journal of Geophysical Research,* vol. 114, no. 5, pp. 1-17.

BUTLER P. G., WANAMAKER A. D., SCOURSE J. D., RICHARDSON C. A. & REYNOLDS D. J. 2011 Long-term stability of δ13C with respect to biological age in the aragonite shell of mature specimens of the bivalve mollusk Arctica islandica, *Palaeogeography, Palaeoclimatology, Palaeoecology,* vol. 302, no. 1-2, pp. 21-30.

BUTLER P. G., WANAMAKER A. D., SCOURSE J. D., RICHARDSON C. A. & REYNOLDS D. J. 2013 Variability of marine climate on the North Icelandic Shelf in a 1357-year proxy archive based on growth increments in the bivalve Arctica islandica, *Palaeogeography, Palaeoclimatology, Palaeoecology,* vol. 373, pp. 141-151.

CARRÉ M., BENTALEB I., BRUGUIER O., ORDINOLA E., BARRETT N. T. & FONTUGNE M. 2006 Calcification rate influence on trace element concetrations in aragonitic bivalve shells: Evidences and mechanisms, *Geochimica et Cosmochimica Acta,* vol. 70, no. 4906-4920.

CARRÉ M., SACHS J. P., PURCA S., SCHAUER A. J., BARACONNOT P., FALCÓN R. A., JULIEN M. L. & LAVALLÉE D. L. 2014 Holocene history of ENSO variance and asymmetry in the eastern tropical Pacific, *Science,* vol. 325, no. 6200, pp. 1045-1048.

CARRÉ M., SACHS J. P., SCHAUER A. J., RODRGUEZ W. E. & RAMOS F. C. 2013 Reconstructing El Ni?o-Southern Oscillation activity and ocean temperature seasonality from short-lived marine mollusk shells from Peru, *Palaeogeography, Palaeoclimatology, Palaeoecology,* vol. 371, pp. 45-53.

CARROLL M. L., JOHNSON B. J., HENKES G. A., MCMAHON K. W., VORONKOV A., AMBROSE JR W. G. & DENISENKO S. G. 2009 Bivalves as indicators of environmental variation and potential anthropogenic impacts in the southern Barents Sea, *Marine Pollution Bulletin,* vol. 59, pp. 193-206.

DETTMAN D. L., FLESSA K. W., ROOPNARINE P. D., SCHÖNE B. R. & GOODWIN D. H. 2004 The use of oxygen isotope variation in shells of estuarine mollusks as a quantitative record of seasonal and annual Colorado river discharge, *Geochimica et Cosmochimica Acta,* vol. 68, no. 6, pp. 1253-1263.

DITTMANN S., RAMSDALE T., KEUNING J., NAVONG N. & BAGGALLEY S. 2013 Benthic Macroinvertebrate Response Monitoring in the Coorong and Murray Mouth, 2012/13. Adelaide.

DIXIT Y., HODELL D. A. & SINHA R. 2015 Oxygen isotope analysis of multiple, single ostracod valves as a proxy for combined variability in seasonal temperature

and lake water oxygen isotopes, *Journal of Paleolimnology,* vol. 53, no. 1, pp. 35-45.

ELLIOT M., WELSH K., CHILCOTT C., MCCULLOCH M., CHAPPELL J. & AYLING B. 2009 Profiles of trace elements and stable isotopes derived from giant long-lived Tridacna gigas bivalves: Potential applications in paleoclimate studies, *Palaeogeography, Palaeoclimatology, Palaeoecology,* vol. 280, no. 1-2, pp. 132-142.

EPSTEIN S., BUCHSBAUM R., LOWNSTAM H. & UREY H. C. 1961 Carbonate-water isotopic temperature scale, *Bulletin of the Geological Society of America,* vol. 62, pp. 417-426.

FERGUSON J., JOHNSON K. R., SANOS G., MEYER L. & TRIPATI A. 2013 Investigating δ13C and Δ14C within *Mytilus californianus* shells as proxies of upwelling intensity, *Geochemistry, Geophysics, Geosystems,* vol. 14, no. 6, pp. 1856-1865.

FINDLATER G., SHELTON A., ROLIN T. & ANDREWS J. 2014 Sodium and strontium in mollusc shells: preservation, palaeosalinity and palaeotemperature of the Middle Pleistocene of eastern England, *Proceedings of the Geologists' Association,* vol. 125, no. 1, pp. 14-19.

FINK D., HOTCHKIS M., HUA Q., JACOBSON G., A.M S., ZOPPI U., CHILD D., MIFSUD C., VAN DER GAAST H., WILLIAMS A. & WILLIAMS M. 2004 The ANTARES AMS facility at ANSTO, *Nuclear instruments and Methods in Physics,* vol. 223-224, pp. 109-115.

FLETCHER M.-S. & THOMAS I. 2010 A quantitative Late Quaternary temperature reconstruction from western Tasmania, Australia, *Quaternary Science Reviews,* vol. 29, pp. 2351-2361.

FLUIN J., HAYNES D. & TIBBY J. 2009 An Environmental History of the Lower Lakes and the Coorong. *In:* DEPARTMENT OF ENVIRONMENT , W.A.N.R (ed.).

GEDDES M. & HALL D. 1990 The Murray. In MACKAY N. & EASTBURN D. eds. The Murray Mouth and Coorong. Canberra: Murray Darling Basin Commision.

GERGIS J., GALLANT A. J. E., BRAGANZA K., KAROLY D. J., ALLEN K., CULLEN L., D'ARRIGO R., GOODWIN I., GRIERSON P. & MCGREGOR S. 2011 On the long-term context of the 1997-2009 'Big Dry' in South-Eastern Australia: insights from a 206-year multi-proxy rainfall reconstruction, *Climatic Change,* vol. 111, no. 3, pp. 923-244.

GILLIKIN D. P., LORRAIN A., BOUILLON S., WILLENZ P. & DEHAIRS F. 2006 Stable carbon isotopic composition of *Mytilus edulis* shells: relation to metabolism, salinity, d13CDIC and phytoplankton, *Organic Geochemistry,* vol. 37, pp. 1371-1382.

GOURAMANIS C., WILKINS D. & DE DECKER P. 2010 6000 years of environmental changes recorded in Blue Lake, South Australia, based on ostracod ecology and valve chemistry, *Palaeogeography, Palaeoclimatology, Palaeoecology,* vol. 297, pp. 223-237.

HENDON H. H., THOMPSON D. W. J. & WHEELER M. C. 2007 Australian rainfall and surface temperature variations associated with the Southern Hemisphere Annular Mode, *Journal of Climate,* vol. 20, pp. 2452-2467.

HOGG A. G., HUA Q., BLACKWELL P. G., NIU M., BUCK C. E., GUILDERSON T. P., HEATON T. J., PALMER J. G., REIMER P. J., REIMER R. W., TURNEY C. S. M. & ZIMMERMAN S. R. H.

2013 SHCal13 Southern Hemispher Calibration, 0-50,000 years cal. BP, *Radiocarbon,* vol. 55, pp. 1889-1903.

JONES D. 1980 Annual cycle of shell growth increment formation in two continental shelf bvalves and its paleoecologic significance, *Paleobiology,* vol. 6, no. 3, pp. 331-340.

KEMP J., RADKE L. C., OLLEY J., JUGGINS S. & DE DECKER P. 2012 Holocene lake salinity changes in the Wimmera, southeastern Australia, provide evidence for millenial-scale climate variability, *Quaternary Reseach,* vol. 77, pp. 65-76.

KOUTAVAS A., DEMENOCAL P. B., OLIVE G. C. & LYNCH-STIEGLITZ J. 2006 Mid-Holocene El Niño–Southern Oscillation (ENSO) attenuation revealed by individual foraminifera in eastern tropical Pacific sediments, *Geology,* vol. 34, no. 12, p. 993.

LAUTENSCHLAGER A. D. 2011 Feeding ecology of benthic invertebrates in an intermittently open estuary. School of life and Environmental Science*.* pp. 169. Deakin University.

LAZARETH C. E., LE CORNEC F., CANDAUDAP F. & FREYDIER R. 2013 Trace element heterogeneity along isochroonous growth layers in bivalve shell: Consequences for environmental reconstruction, *Palaeogeography, Palaeoclimatology, Palaeoecology,* vol. 373, pp. 39-49.

LAZARETH C. E., VANDER PUTTEN E., ANDRÉ L. & DEHAIRS F. 2003 High-resolution trace element profiles in shells of the magrove bivalve *Isognomon ephippium*: a record of environmental spatio-temporal variations?, *Estuarine, Coastal and Shelf Science,* vol. 57, pp. 1103-1114.

LÉCUYER C., HUTZLER A., AMIOT R., DAUX V., GROSHENY D., OTERO O., MARTINEAU F., FOUREL F., BALTER V. & REYNARD B. 2012 Carbon and oxygen isotope fractionations between aragonite and calcite shells from modern molluscs, *Chemical Geology,* vol. 332-333, pp. 92-101.

MATTHEWS T. G. & CONSTABLE A. J. 2004 Effect of flooding on estuarine bivalve populations near the mouth of the Hopkins River, Victoria, Australia, *Journal of the Marine Biological Association of the United Kingdom,* vol. 84, pp. 633-639.

MCGREGOR H., TIMMERMANN A. & TIMM O. 2010 A unified proxy for ENSO and PDO variability since 1650, *Climate of the Past,* vol. 6, no. 1, pp. 1-17.

MCKIRDY D. M., THORPE C. S., HAYNES D. E., GRICE K., KRULL E., HALVERSON G. P. & WEBSTER L. J. 2010 The biogeochemical evolution of teh Coorong during the mid- to late Holocene: An elemental, isotopic and biomarker perspective, *Organic Geochemistry,* vol. 41, pp. 96-110.

MOROS M., DE DECKER P., JANSEN E., PERNER K. & TELFOD R. J. 2009 Holocene climate variability in the Southern Ocean recorded in a deep-sea sediment core off South Australia, *Quaternary Science Reviews,* vol. 28, pp. 1932-1940.

NEUKOM R. & GERGIS J. 2011 Southern Hemisphere high-resolution palaeoclimate records of the last 2000 years, *The Holocene,* vol. 22, no. 5, pp. 501-524.

O'NEIL D. D. & GILLIKIN D. P. 2014 Do freshwater mussel shells record road-salt pollution?, *Scientific Reports,* vol. 4, p. 7168.

PAOULAIN C., GILLIKIN D. P., THÉBAULT J. M., MUNARON M. B., ROBERT R., PAULET Y.-M. & LORRAIN A. 2015 An evaluation of Mg/Ca, Sr/Ca and Ba/Ca ratios as

environmental proxies in aragonite bivalve shells, *Chemical Geology,* vol. 396, pp. 42-50.

PEARCE N. J., PERKINS W. T., WESTGATE J. A., GORTON M. P., JACKSON S. E., NEAL C. L. & CHERNERY S. P. 1997 A compilation of new and published major and trace element data for NIST SRM 610 and NIST SRM 612 glass reference materials, *Geostandards Newsletter,* vol. 21, no. 1, pp. 115-144.

PRENDERGAST A. L., STEVENS R. E., BARKER G. & O'CONNELL T. C. 2015 Oxygen isotope signitures from land snail (*Helix malanostoma*) shells and body fluid: Proxies for reconstructing Mediterranean and North African rainfall, *Chemical Geology,* vol. 409, pp. 87-98.

REIMER P. J., BARD E., BAYLISS A., BECK J. W., BLACKWELL P. G., BRONK RAMSEY C., BUCK C. E., EDWARDS R. L., FRIEDRICH M., GROOTES P. M., GUILDERSON T. P., HAFLIFASON H., HAJDAS I., HATTÉ C., HEATON T. J., HOFFMANN D. L., HOGG A. G., HUGHEN K. A., KAISER K. F., KROMER B., MANNING S. W., NIU M., REIMER R. W., RICHARDS D. A., SCOTT E. M., SOUTHON J. R., TURNEY C. S. M. & VAN DER PLICHT J. 2013 IntCal13 and Marine13 radiocarbon age calibration curves, 0-50,000 years cal BP, *Radiocarbon,* vol. 55, no. 1869-1887.

SAMPEI Y., MATSUMOTO E., DETTMAN D. L., TOKUOKA T. & ABE O. 2005 Paleosalinity in a brackish lake during the Holocene based on stable oxygen and carbon isotops of shell carbonate in Nakaumi Lagoon, southwest Japan, *Palaeogeography, Palaeoclimatology, Palaeoecology,* vol. 224, no. 352-366.

SAUNDERS K. M., GROSJEAN M. & HODGSON D. A. 2013 A 950 yr temperature reconstruction from Duckhole Lake, southern Tasmania, Australia, *The Holocene,* vol. 23, no. 6, pp. 771-783.

SAUNDERS K. M., KAMENIK C., HODGSON D. A., HUNZIKER S., SIFFERT L., FISCHER D., FUJAK M., GIBSON J. A. E. & GROSJEAN M. 2012 Late Holocene changes in precipitation in northwest Tasmania and their potential links to shifts in the Southern Hemisphere westerly winds, *Global and Planetary Change,* vol. 92-93, pp. 82-91.

SCHÖNE B. R., DUNCA E., FIEBIG J. & PFEIFFER M. 2005 Mutvei's solution: An ideal agent for reslving microgrowth structures of biogenic carbonates, *Palaeogeography, Palaeoclimatology, Palaeoecology,* vol. 228, no. 149-166.

SCHÖNE B. R. & FIEBIG J. 2009 Seasonality in the North Sea suring the Allerød and Late Medieval Climate Optimum using bivalve sclerochronology, *International Journal of Earth Sciences,* vol. 98, pp. 83-98.

SCHÖNE B. R., RADERMACHER P., ZHANG Z. & JACOB D. E. 2013 Crystal fabrics and element impurities (Sr/Ca, Mg/Ca and Ba/Ca) in shells of *Arctica islandica* - implications for paleoclimate reconstructions, *Palaeogeography, Palaeoclimatology, Palaeoecology,* vol. 373, pp. 50-59.

SCHÖNE B. R. & SURGE D. 2014 Bivalve shells: ultra high-resolution paleoclimate archives, *Pages,* vol. 22, no. 1, pp. 20-21.

SCHÖNE B. R., ZHANG Z., JACOB D. E., GILLIKIN D. P., TÜTKEN T., GARBE-SCHÖNBERG D., MCCONNAUGHEY T. & SOLDATI A. 2010 Effect of organic matrices on the determination of the trace element chemistry (Mg, Sr, Mg/Ca, Sr/Ca) of aragonitic bivalve shells (*Arctica islandica*) - comparison of ICP-OES and LA-ICCP-MS data, *Geochemical Journal,* vol. 44, pp. 23-37.

SNYDER C. W. 2010 The value of paleoclimate research in our changing climate, *Climatic Change,* vol. 100, pp. 407-418.

SURGE D. & LOHMANN K. C. 2008 Evaluating Mg/Ca ratios as a temperature proxy in the estuarine oyster, *Crassostrea virginica*, *Journal of Geophysical Research,* vol. 113, pp. 1-9.

THOMLINSON G. W. 1996 The upper southeast dryland and flood management plan. Freshwater inflows to the Coorong South Lagoon. Adelaide: Natural Resources Council of South Australia.

THOMPSON I., JONES D. S. & DREIBELBIS D. 1980 Annual internal growth banding and life history of the ocean quahog *Artica islandica* (Mollusca: Bivalvia), *Marine Biology,* vol. 57, pp. 25-34.

TULIPANI S., GRICE K., KRULL E., GREENWOOD P. & REVILL A. T. 2014 Salinity variations in the norther Coorong Lagoon, South Australia: Significant changes in the ecosystem following human alteration to the natural water regime, *Organic Geochemistry,* vol. 75, pp. 74-86.

UREY H. C. 1947 The thermodynamic properties of isotopic substances, *Journal of the Chemical Society*, no. 0, pp. 562-581.

VAN ACHTERBERGH, RYAN C., JACKSON S. E. & GRIFFIN W. L. 2001 Appendix 3 data reduction software LA-ICP-MS. In SYLVESTER P. J. ed. Laser Ablation ICP-MS in teh Earth Sciences*.* pp. 239-243.

VERSTEEGH E. A. A., TROELSTRA S. R., VONHOF H. B. & KROON D. 2009 Oxygen isotope composition of bivalve seasonal growth increments and ambient water in the rivers Rhine and Meuse, *Palaios,* vol. 24, pp. 497-504.

WANAMAKER A. D., KREUTZ K. J., SCHÖNE B. R., MAASCH K. A., PERSHING A. J., BORNS H. W., INTRONE D. S. & FEINDEL S. 2009 A late Holocene paleo-productivity record int he western Gulf of Maine, USA, inferred from growth histories of the long-lived ocean quahog (*Arctica isalandica)*, *International Journal of Earth Sciences,* vol. 98, pp. 19-29.

WELLS F. E. & THRELFALL T. J. 1982 Salinity adn temperture tollerance of *Hydrococcus brazieri* (T. Woods, 1876) and *Arthritica semem* (Menke, 1843) from the Peel-Harvey estuarine system, Western Australia, *Journal of the Malacological Society of Australia,* vol. 5, pp. 151-156.

WITBAARD R., DUINEVELD G. C. A. & DE WILDE P. 1997 A long-term growth record derived from *Arctica islandica* (Mollusca, Bivalvia) from the Fladen Ground (Northern North Sea), *Journal of the Marine Biological Association of the United Kingdom,* vol. 77, pp. 801-816.

WURSTER C. M. & PATTERSON W. P. 2001 Seasonal variation in stable isotope oxygena dn carbon values recovered from modern lacustrine freshwater molluscs: Paleoclimatological implications for sub-weekly climate records, *Journal of Paleolimnology,* vol. 26, no. 205-218.

YAN H., CHEN J. & XIAO J. 2014 A review on bivalve shell, a tool for reconstruction of paleo-climate and paleo-environment, *Chinese Journal of Geochemistry,* vol. 33, no. 3, pp. 310-315.

APPENDIX A: STABLE ISOTOPE RAW DATA

Stable isotope measurements from 5-shell composite and replicate individuals.

Depth	$\delta^{18}O$	$\delta^{13}C$	$\delta^{18}O_{aragonite}$	$\delta^{13}C_{aragonite}$
5	5.22	1.09	4.85	0.14
6	5.74	0.43	5.37	-0.52
7	5.67	0.12	5.3	-0.83
8	5.45	0.7	5.08	-0.25
9	5.24	-0.04	4.87	-0.99
10	5.88	0.61	5.51	-0.34
11	5.75	0.94	5.38	-0.01
12	5.48	0.56	5.11	-0.39
13	5.82	0.42	5.45	-0.53
14	5.19	0.02	4.82	-0.93
15	5.35	0.41	4.98	-0.54
16	5.88	0.11	5.51	-0.84
17	5.25	0.46	4.88	-0.49
18	5.14	0.79	4.77	-0.16
19	5.49	0.5	5.12	-0.45
20	5.29	-0.32	4.92	-1.27
21	5.33	1.02	4.96	0.07
22	5.07	0.51	4.7	-0.44
23	4.89	0.45	4.52	-0.5
24	4.11	0.81	3.74	-0.14
25	5.4	0.35	5.03	-0.6
26	5.46	0.76	5.09	-0.19
27	5.07	-0.36	4.7	-1.31
28	5.28	1.27	4.91	0.32
29	5.19	0.53	4.82	-0.42
30	4.67	0.78	4.3	-0.17
31	5.12	0.77	4.75	-0.18
32	4.3	0.91	3.93	-0.04
33	5.15	-0.13	4.78	-1.08
34	5.45	0.76	5.08	-0.19
35	4.46	1.45	4.09	0.5
36	4.71	0.37	4.34	-0.58
37	5.22	0.91	4.85	-0.04
38	4.5	0.24	4.13	-0.71
39	4.93	0.31	4.56	-0.64
40	4.88	0.76	4.51	-0.19
41	4.92	0.08	4.55	-0.87
42	4.96	0.36	4.59	-0.59
43	5.04	0.47	4.67	-0.48

44	4.83	0.56	4.46	-0.39
45	5.34	0.84	4.97	-0.11
46	5.01	1.42	4.64	0.47
47	4.5	-0.07	4.13	-1.02
48	4.65	0.35	4.28	-0.6
49	4.73	0.87	4.36	-0.08
50	4.77	0.81	4.4	-0.14
51	4.97	0.54	4.6	-0.41
52	4.57	1.58	4.2	0.63
53	4.54	-0.18	4.17	-1.13
54	4.23	2.03	3.86	1.08
55	4.78	0.19	4.41	-0.76
56	4.59	0.02	4.22	-0.93
57	4.32	0.1	3.95	-0.85
58	4.22	0.84	3.85	-0.11
59	4.85	0.79	4.48	-0.16
60	5.18	1.57	4.81	0.62
61	6.04	1.5	5.67	0.55
62	4.72	-0.17	4.35	-1.12
63	4.98	-0.47	4.61	-1.42
64	4.52	0.51	4.15	-0.44
65	5.27	1.36	4.9	0.41
66	4.7	0.2	4.33	-0.75
67	4.69	-0.42	4.32	-1.37
68	4.97	0.65	4.6	-0.3
69	4.93	0.54	4.56	-0.41
70	4.09	-0.42	3.72	-1.37
71	4.07	-0.31	3.7	-1.26
72	4.58	0.59	4.21	-0.36
73	4.45	1.3	4.08	0.35
74	4.82	0.72	4.45	-0.23
75	5.12	-0.28	4.75	-1.23
77	4.73	0.27	4.36	-0.68
78	4.24	0.17	3.87	-0.78
79	4.9	0.35	4.53	-0.6
80	4.19	0.17	3.82	-0.78
81	4.33	0.21	3.96	-0.74
82	4.96	0.86	4.59	-0.09
83	5.53	0.57	5.16	-0.38
84	5.21	0.85	4.84	-0.1
85	5.56	0.88	5.19	-0.07
86	5.16	0.02	4.79	-0.93
87	5.04	0.78	4.67	-0.17
88	5.23	0.9	4.86	-0.05

89	5.52	0.39	5.15	-0.56
90	5.69	1.25	5.32	0.3
91	4.93	0.38	4.56	-0.57
92	4.94	0.94	4.57	-0.01
93	5.49	1.05	5.12	0.1
94	5.75	1.27	5.38	0.32
95	5.52	0.12	5.15	-0.83
96	5.27	0.69	4.9	-0.26
97	5.78	1.03	5.41	0.08
98	5.14	0.53	4.77	-0.42
99	5.04	0.16	4.67	-0.79
100	4.55	0.33	4.18	-0.62
101	5.5	-0.29	5.13	-1.24
102	4.55	-0.41	4.18	-1.36
103	5	0.33	4.63	-0.62
104	4.41	0.2	4.04	-0.75
105	4.87	0.65	4.5	-0.3
106	4.77	1.03	4.4	0.08
107	5.27	1.16	4.9	0.21
108	5.35	0.71	4.98	-0.24
109	5.35	0.88	4.98	-0.07
110	4.8	2.08	4.43	1.13
111	5.26	0.31	4.89	-0.64
112	4.9	0.82	4.53	-0.13
113	5.15	0.89	4.78	-0.06
114	5.01	0.61	4.64	-0.34
115	5.11	2.27	4.74	1.32
117	5.13	1.07	4.76	0.12
118	5.26	1.39	4.89	0.44
119	5.12	0.47	4.75	-0.48
120	4.85	0.72	4.48	-0.23
121	4.89	1.09	4.52	0.14
122	5.3	0.15	4.93	-0.8
123	5	0.36	4.63	-0.59
124	4.26	0.36	3.89	-0.59
125	4.76	0.42	4.39	-0.53
126	4.48	2.52	4.11	1.57
127	5.08	0.9	4.71	-0.05
128	5.09	1.04	4.72	0.09
129	5.09	1.1	4.72	0.15

APPENDIX B: TRACE ELEMENT RAW DATA

SOLUTION ICP-MS

Raw output in ppb for Mg, Sr and Ba measured on 5-shell composite carbonate. Following this analysis, standards were found to be 10 times higher than thought and so raw data was divided by 10 to account for the error in calibration. Please see Appendix C (electronic) for other elements and worked data.

Core depth	24 Mg [2]		88 Sr [2]		137 Ba [2]	
	Conc. [ppb]	Conc. RSD	Conc. [ppb]	Conc. RSD	Conc. [ppb]	Conc. RSD
5	3.00015912	2.161351673	22.05622586	3.452458445	2.685533418	4.049687682
6	1.437841706	4.558133547	9.897459374	0.41166901	0.995517165	1.327611499
7	1.964857796	1.412448934	17.35629225	2.390332277	2.381868557	0.402415417
8	0.744749778	0.434505532	5.801934905	1.655139051	0.689314601	0.426164063
9	0.938459823	5.526947385	5.608129119	2.473319682	0.573967067	1.481813733
10	6.400075805	2.524356128	14.75754756	1.342157268	2.186175689	2.814559539
11	3.393099264	1.906173588	22.22780504	1.02838781	1.390661762	0.3479684
12	2.84061296	2.845904305	25.0003996	1.546393564	3.897791703	1.465175399
13	3.999365075	2.950488748	32.79621661	1.952782098	1.811229903	1.021277168
14	3.2125412	4.562877562	29.93172273	2.882851601	2.310070147	3.478699196
15	7.229816378	3.873376177	55.31632488	1.357002578	3.774521192	1.344768777
16	4.049208109	2.762622845	28.45882465	1.417399175	2.101725289	0.236415093
17	2.550870782	1.101988924	30.83707129	0.282051201	1.751187424	2.052259363
18	4.490469816	2.328673595	30.8825407	0.273624515	4.388226265	1.24080383
19	5.560122193	2.600938897	51.48256801	1.257794825	1.446308738	2.046144316
20	2.240239124	1.220977732	23.0460274	0.982202998	1.792132599	1.244182044
23	3.638870363	2.905131303	29.78035921	1.330276419	1.560235402	1.41436443
24	2.119434434	1.704209077	23.60535912	1.166519936	1.223564254	0.68716647
24	4.785752763	12.29373042	54.30005365	11.90577713	1.438036055	12.36788555
24	18.60504367	6.539693112	30.70905913	5.66125707	1.320252263	5.297720652
25	1.773549215	3.766862993	15.94850057	1.695420905	1.684366879	0.555820743
26	3.237241692	2.364095393	31.25862058	0.964271744	0.985085454	1.448526604
27	3.068066891	3.180785872	21.15318029	3.555934225	1.587899817	1.021528555
28	2.364259083	2.844891685	20.0952591	1.181252272	1.473885679	0.960416065
29	5.13649722	2.65170724	46.03172602	2.772207175	2.179412549	2.876043076
30	2.405038024	2.093688954	12.9008392	0.600481642	0.703175835	1.451988917
31	12.19429962	2.425159363	49.17699118	1.289202037	1.008264578	0.934261323
32	2.141149737	4.162922403	11.49705381	0.653809551	0.769332158	6.281483305
33	4.170431888	1.859239782	28.18436403	0.867717784	0.870821129	0.4632807
34	3.284854579	4.076207419	13.85579305	2.598875923	0.983108892	1.973308408
36	6.629588801	2.603947533	49.72235402	0.820112974	2.798641645	1.947504117
37	5.255323376	3.872481048	25.3980023	1.327125891	1.280513298	2.687023589
38	1.974000589	3.970500681	11.81974438	0.634072619	1.632950833	0.238074975
39	3.210280505	1.846902186	16.83874321	0.571637905	1.857376442	0.937680491
40	9.096047663	2.212899882	13.84095277	0.664590191	1.32146662	2.831813716
41	5.094867607	2.91153886	25.9648861	0.944838186	0.931291447	1.07321215
42	2.991325567	0.641508068	16.33889084	0.686849853	0.551354048	2.313882958
43	5.441795972	4.114113635	24.04598016	3.321702347	1.312243064	2.847473628
44	3.891755126	3.996128364	25.63040238	2.014839986	1.437339148	1.801418979
45	5.693818592	2.563483119	43.95063581	1.071212208	1.948592189	1.499717046
46	2.698222476	1.418848075	15.12395535	1.556549469	1.01728825	3.172573086
47	4.843617589	7.227704623	32.40506968	7.566619628	0.705500297	8.414986746

48	5.700803016	2.986391876	32.20181907	2.416011802	1.408882697	3.082117397
49	7.942997132	4.695159878	56.44139484	3.758134424	1.9176075	3.859730657
50	6.73153149	10.51844614	31.44103237	8.928235446	1.508005208	9.531657782
51	6.889975798	13.73526322	45.93836204	12.4424769	1.438993353	12.74214846
52	2.256047396	2.608087912	15.70046762	0.813541262	0.817961492	1.272486169
53	6.044123083	2.811482648	46.36365836	0.853027204	1.136333731	6.948330023
54	3.12543974	2.632339256	17.9602012	0.926906921	0.696632058	1.863844405
54	2.761152987	2.432310888	20.6985209	0.733572325	0.981423038	1.671595164
55	8.206717901	2.080473018	16.73354485	1.823223406	1.51281523	1.441819109
56	5.910029898	1.390423912	31.29484646	0.567282248	0.965386822	2.66693621
57	2.994691908	2.072910255	16.04582759	0.705261647	1.133675607	2.097796512
58	3.444901599	4.071958797	23.34092217	1.355079697	1.34298901	1.599749844
59	5.995260381	1.574165423	28.71366066	0.77645489	1.278996818	1.907118382
62	4.51022008	0.575138515	19.2031173	1.720376185	0.750826302	0.824777368
63	2.301313615	2.562715644	15.14175368	0.412531552	0.561019534	1.055402561
64	1.806574353	2.78983402	12.62111577	1.260100507	0.853278116	1.766556619
65	4.558337408	1.062767552	25.61420328	0.375421776	0.821949175	0.099316768
66	6.09379402	3.585728093	27.87671413	2.9127554	1.243886732	4.758060052
67	2.050746693	6.901076753	18.72496928	3.786280359	1.028231605	3.243672768
68	3.649843046	0.90901743	26.86503994	3.462398785	1.193184538	2.827666705
69	5.103163393	2.137885726	23.63553338	0.402814742	1.14155855	2.149989959
70	5.726163177	2.374609435	48.46186102	1.348915904	2.138783683	1.095008967
71	4.699722071	1.743220647	48.77078277	1.334457901	1.884204225	1.775103829
72	5.675865221	4.298453271	30.25678617	4.349054705	1.430203651	4.120087149
78	2.772229123	0.489570733	10.86166035	0.626766884	0.622357681	0.943979299
79	2.483113441	1.002585943	15.31132733	0.672313484	0.441293463	4.235889307
81	6.656543082	1.759269421	41.32780022	0.572241166	1.704447907	1.613720882
82	3.843262858	1.327584587	30.16328772	1.516584552	0.968462642	1.450120116
82	3.16030518	9.325435086	24.82260781	9.729376326	0.836550721	9.81540755
83	6.532660193	2.145612285	46.94863289	0.70495073	2.449155785	1.130292154
84	1.944155352	2.575620936	3.603362832	1.541734168	0.166620163	5.820666104
85	1.106752182	4.709769861	7.33586323	0.76221711	0.282127387	6.21443064
86	4.234877823	2.65009666	23.23907896	3.004599952	0.896861371	2.890692102
87	3.53230037	3.740335785	23.45541096	1.810399292	0.753968191	1.754760971
88	8.438161386	9.040101803	68.29143554	8.928193968	1.778302539	7.906467625
89	3.433037627	1.787975591	27.56570158	0.97582048	1.093856548	1.593501366
90	3.026681084	5.082199233	22.62758525	2.273948224	1.551935993	2.463943835
91	4.049039036	0.643641065	33.6247142	1.80080065	0.641622031	3.594206631
92	0.903220567	4.834453063	4.068448189	3.529157822	0.085968875	2.032758294
92	1.540724615	2.958196779	5.531778166	1.190833797	0.274181063	1.692994136
93	6.582722267	0.398769197	41.99841208	1.284874267	0.917777181	0.693039968
94	8.723277051	0.790605205	60.88337132	1.850314814	1.535149706	2.306138781
95	1.173290828	5.283576411	6.836863996	1.679031226	0.44340476	2.072738097
96	4.871003115	2.538695486	42.78663652	1.150333369	1.398635599	5.038474818
97	0.727612905	6.554906998	6.186131546	2.237198333	0.224651781	4.12257056
98	1.868864308	0.666802154	9.352965033	1.953417037	0.172889808	6.408918985
99	4.708137137	3.778308996	32.76361212	2.125211679	1.370923284	0.736066453
99	0.720959257	1.372587179	4.259082269	0.742579925	0.174737823	1.955265247
100	6.768665819	0.922966767	55.01989474	1.53489041	1.044732986	1.081109436
101	5.339271927	6.510816049	16.85261795	6.167153123	0.365884296	6.828967089
102	2.115489186	1.681783757	20.20306616	0.895144152	0.529269268	1.528796501
103	2.169065519	0.903987757	17.60586554	1.081371259	0.829152508	9.525578674
104	1.130419671	4.982356151	8.561136585	0.442010128	0.532609635	1.012706824
105	1.691514421	2.78476219	12.47494701	0.684755441	0.505089541	4.27859426
106	7.046724051	0.761539781	56.53646068	0.493262997	1.229719552	0.332129244

107	4.703905263	2.008084423	10.78204518	1.2264325	0.260350563	2.03006375
108	3.186636732	2.434920526	8.642519044	1.298622943	0.754034139	0.233892159
108	2.088312143	1.123434941	12.04504591	0.562778724	0.585463251	0.696725462
109	3.397878009	2.883837289	16.85253389	2.338686698	0.524156899	2.965707903
110	3.595474933	6.290147599	31.04586759	6.018975748	1.744628046	4.934278614
111	6.090527206	4.179291981	19.09033797	2.124294729	1.300589293	2.197222648
112	2.495665231	0.999971298	18.78139652	1.167386963	0.544500021	0.529897089
113	4.650476319	1.52501487	28.26033518	3.040258036	0.792245765	1.413086361
114	2.328476693	3.037779696	14.86981241	0.93189391	0.645915694	1.291841526
114	4.973362005	1.252692957	29.64487857	0.6003995	1.062662629	0.662989609
115	4.548324746	2.936043546	32.14228138	0.50822315	1.27489185	1.663420537
117	3.460776171	0.730134892	22.138313	0.592886245	0.480896016	2.413792769
119	2.870095692	4.649212745	21.22541068	5.199333441	1.32401418	4.634504183
119	2.698197986	4.318806979	20.58060128	2.764441944	1.042746011	2.873035393
120	3.188732245	0.424732624	15.23792931	1.893153698	0.396042487	7.22845136
121	1.949377705	7.389639742	12.02844874	2.759852797	2.09265395	3.357416675
122	2.269890307	3.72279156	15.96708278	1.581436171	1.050036487	2.671249129
123	3.168841167	3.28469632	21.48441962	0.382838745	0.637396853	2.330778011
124	1.304160591	4.520228587	10.00236529	2.408343657	0.812225595	1.240625065
125	5.020175625	3.876469864	9.304504123	0.930489106	0.737680929	1.399233776
126	4.019832221	5.759932867	29.90587201	5.285850117	1.038844649	6.945836605
127	7.518748669	4.378426186	21.36171172	4.553961854	1.134297154	2.747042136
128	1.575467415	0.834673025	12.06160176	1.26625716	0.983906989	2.575523889
129	1.64481895	7.493510189	11.91539424	7.513262172	0.633214616	8.822428214

LA-ICP-MS

LA-ICP-MS was performed on slides C18.1 and C18.4. Boxes in red highlight shells that were not included in the analyses as they were determined either visually, or by elevated indium to have missed the shell carbonate. During analysis, slide movement within the ablation chamber caused transects to deviate from the set course. This was due to trial and error methods of adhering the slide within the chamber as a purpose built holder was not available. For LA-ICP-MS standards, transformations and raw data please see Appendix C (electronic).

101	102	103	104
301	302	303	304
501	502	503	504
701	702	703	704
891	892	893	894
1101	1102	1103	1104
121	122	123	124
305	306	307	308
505	506	507	508
705	706	707	708
895	896	897	898
1105	1106	1107	1108

C18.1

21l	21m	21n	
21o	21p	21q	
21r	21s	21t	21u
21v	21w	21x	
21y	21z	21aa	21bb
21cc	21dd	21ee	
	21ff		

C18.4

APPENDIX C: ELECTRONIC TRACE ELEMENTAL DATA

Appendix C contains the spread sheets of all trace elemental data in a raw and worked form. An electronic copy is with the supervisors of this project.